Macromolecules
ARTICLE

Macromolecules **2010**, *43*, 1467–1472 **1467**
DOI: 10.1021/ma902433v

Aggregation of Carbon Nanotubes in Semidilute Suspension

Ludovic Moreira,[†] René Fulchiron,[†] Gérard Seytre,[†] Philippe Dubois,[‡] and Philippe Cassagnau*,[†]

[†]*Université de Lyon, Lyon, F-69003, France, Université de Lyon 1, Lyon, F-69622, France, CNRS UMR5223, Ingénierie des Matériaux Polymères: Laboratoire des Matériaux Polymères et Biomatériaux, F-69622 Villeurbanne (France) and* [‡]*Center of Innovation and Research in Materials & Polymers (CIRMAP), Laboratory of Polymeric and Composite Materials, University of Mons-UMONS, Place du Parc 20, B-7000 Mons (Belgium)*

Received November 3, 2009; Revised Manuscript Received December 24, 2009

ABSTRACT: The CNTs aggregation in a low-viscosity PDMS matrix was studied from simultaneous time-resolved measurements of electrical conductivity and dynamic shear modulus. The concentration of nanotubes (ϕ = 0.2%) was chosen in order to be in the semidilute regime of the suspensions. After a nonlinear compressive deformation, it was shown that the kinetics of CNTs aggregation strongly depend on the amplitude of the dynamic shear deformation. Actually, the kinetics of aggregation develops rapidly by increasing the deformation. However, above a critical deformation (γ_c = 60% corresponding to a critical Peclet number $Pe_c \approx 1 \times 10^4$), the equilibrium value of the storage modulus and electrical conductivity decreases with increasing the deformation. It was then concluded that low shear deformations induced an aggregation mechanism, but these aggregates broke down at high shear, forming small aggregates with less entanglements. Furthermore, this phenomenon of CNTs cluster aggregation was also highlighted by optical microscopy as the clustering mechanism of the CNTs was clearly observable after few hours.

Introduction

Over the past decade, polymer composites based on carbon nanotubes (CNTs) have been extensively investigated due to their specific properties. CNTs can be viewed as one-dimensional nanomaterial as they possess a very high aspect ratio (generally higher than 100 for a tube-diameter usually lower than 10 nm). However, the successful development of CNTs-based composites requires controlling the dispersion of CNTs within the polymer matrix. Indeed, CNTs have strong tendency to agglomerate in densely packed bundles and different strategies have been then developed to optimize CNTs dispersion in, e.g., thermoplastic polymers. A direct consequence of the incorporation of CNTs in molten polymers is the significant change in the viscoelastic and electrical properties. Compared with common particles, the large aspect ratio of CNTs leads to the formation of a solid-like material at a relatively low nanotubes concentration. The concentration onset, at which the viscoelastic and electrical properties dramatically change is referred in the literature as the percolation threshold p_c. Beyond the percolation threshold a fractal nanotubes network arises and dominates the rheological responses[1−11] and electrical properties.[3,6,9,12−14] Recently, Kayatin and Davis[15] showed two separate subtypes of rheological response: A developing nanotubes network was suggested at low frequencies whereas a saturated elastic network was observed at higher concentration. Interestingly these authors also proved that the surface chemistry of CNTs plays a dominant role in their reaggregation. However, we pointed out[16] from a viscoelastic point of view that the fractal criterion of self-similar relaxation associated with the percolation threshold (liquid-like to solid-like transition) cannot be rigorously applied to CNTs-based suspensions. On the other hand, some work[17,18] in the literature reported a reduced viscosity of polymer nanocomposites at low filler concentrations. This striking phenomenon was also observed in some polymer/CNTs composites[6,19] in the semidilute regime. Generally speaking, this apparent violation of the Einstein law is discussed in terms of the modification of the longest relaxation times (constraint release mechanism) induced by the presence of nanoparticles.

On the other hand, the dispersion and the anisotropy (alignment or packing) of nanotubes have a strong influence on the rheological, electrical, and mechanical properties of the nanocomposites. Actually it is expected that the high aspect ratio of CNTs combined with intensive flows leads to anisotropy of carbon nanotubes suspensions. This was clearly demonstrated by the group of Hobbie from optical measurements (birefringence and dichroism experiments) on sheared semidilute)[20−23] and dilute (combined with small-angle scattering[24] suspensions of carbon nanotubes. Interestingly, these authors showed that for weakly elastic fluids (viscous polymer) and at low shear stress nanotubes orient along the direction flow. However a transition to vorticity alignment was observed above a critical shear stress corresponding to a critical Deborah number of approximately 0.15. Note that the Deborah number is also called the Weissenberg number in viscoelasticity or the Peclet number (*De* or $We = \tau\dot{\gamma}$ where τ and $\dot{\gamma}$ denote relaxation time and shear rate respectively). On the contrary, for highly elastic polymer solutions (Boger fluids) nanotubes orient with the flow field at high shear rates. Qualitatively, these results are in agreement with the theoretical studies of fiber and/or rod orientation in viscoelastic fluid under shear flow. On the other hand, Chatterjee and Krishnamoorti[25] studied the rheological response of single-wall carbon nanotubes dispersed in poly(ethylene oxide) showed that under steady shear, the CNT flocks locally rearrange in response to the applied deformation and results in cluster−cluster jamming (network formation) that gives rise to a stress overshoot (transient regime). With continuous shearing the fractal network

*Corresponding author. E-mail: philippe.cassagnau@univ-lyon1.fr.

Published on Web 01/07/2010

breaks up and the suspension flows until the final steady state, i.e., the equilibrium between breakup and bond formation of CNT flocks. Surprisingly enough, some development of intriguing structures of CNTs aggregates under shear flow have been optically observed. Hobbie and Fry[26] reported a flow regime where banding of CNTs was observed in polysobutylene suspensions. Ma et al.[27] observed that CNTs aggregates in an epoxy resin can form, under controlled gap size and low shear rate, unusual helical bands that are aligned perpendicular to the shear flow.

From processing and qualitative points of view, the extrusion conditions have been shown to strongly influence the dispersion of nanotubes and following this, the electrical properties.[28,29] The influence of shear-induced nanotubes orientation on electrical conductivity property has been first reported by Kharchenko et al.[5] from simultaneous measurements of electrical and rheological properties. They observed the decrease of the viscosity and electrical conductivity with increasing shear rate ($0.001 < \dot{\gamma}(s^{-1}) < 10$). As explained by the authors, the conductivity is reduced as the tube−tube contacts decrease with the orientation of nanotubes induced by the shear in the flow field. This phenomenon was also reported for fractal flocks such as carbon black.[30] However, owing to low aspect ratio of carbon black these effects are observed at much higher concentration than in the carbon nanotubes systems. Another interesting feature of nanocomposites under flow, is the subsequent formation of the percolative network in the melt during annealing or rest time after flow cessation. Alig et al.[29,31] and Obrzut et al.[32] have reported on the electrical-conductivity recovery (or network formation) of polymer nanocomposites filled with CNTs. In their recent paper, Alig et al.[33] studied the kinetic of breaking and reforming of a conductive CNTs network in a polycarbonate matrix by simultaneous time-resolved measurements of electrical conductivity and dynamic shear modulus. They pointed out that the recovery (after shear cessation) of both electrical and mechanical properties is attributed to the reformation of the network of interconnected nanotubes cluster (mechanism of cluster aggregation). Qualitatively, these results agree with the conclusions of the work of Chatterjee and Krishnamoorti[25] on the dynamic of break up and formation of the CNTs network.

Finally as pointed out by Huang et al.,[34] the main questioning aspect rising from some of these studies is the state of nanotubes dispersion in many rheological experiments. Apart from the aspect of CNTs dispersion in a polymer matrix, a rheological experiment needs first to prepare a sample. Depending on the polymer matrix different processes can be used such as: injection molding, pressing and solvent/evaporation. Furthermore, the crystalline transition for semicrystalline polymers and associated phase separation inducing filler migration is another important step in the sample memory. Finally, the sample must be placed between the cell of the rheometer and consequently it is submitted to additional stress and deformation (extensional deformation generally) and heating in most of the cases.

In a general framework of the rheology of the CNTs suspensions in semidilute regime, the present work aims to study the aggregation mechanism of a CNTs network (untreated nanotubes) in PDMS matrix. The main part of this work is devoted to the influence of the amplitude of dynamic shear conditions on the viscoelastic and electrical properties of PDMS/CNTs suspension. This objective was achieved by simultaneous time-resolved measurements of electrical conductivity and dynamic shear modulus.

Materials, Methods, and Background

The first challenge in nanocomposite preparation is to separate the nanotubes from their initial aggregation assemblies (bundles at the mircoscale). For this purpose, we used a polydimethylsiloxane (PDMS)/CNTs suspension developed by Beigbeder et al.[35] based on untreated nanotubes since our objective is to study the nanotubes dynamics for the network formation. From experimental and theoretical results, these authors demonstrated that the CH-π interactions between the PDMS methyl groups and the π-electron rich surface of multiwall nanotubes (MWNT) are favorable to CNTs dispersion in PDMS at the level of individual CNTs. Consequently, PDMS/MWNT nanocomposite is a relevant system to study dynamics of CNTs in semidilute suspensions. In the present study, multiwall carbon nanotubes with a diameter of $d \approx 10$ nm, average length of $L \approx 1.5\,\mu$m and a purity of mininimum 90% were investigated. The aspect ratio L/d of these MWCNTs is then around 160. Furthermore, these MWCNTs have never undergone any surface treatment after being produced by CCVD and were directly used as masterbatch predispersed in PDMS (containing 0.5 wt % in MWCNTs) using a high shear industrial dispersion process and supplied under Biocyl 2000 trade name by Nanocyl SA (Sambreville, Belgium).

Polydimethylsiloxane (PDMS) Sylgard 184-Part A (from Dow Corning, USA) was used as silicone sample. The number-average molar mass of this PDMS sample is $M_n = 32\,000\ g\cdot mol^{-1}$. According to literature,[36] this molar mass is close to the critical molar mass for the viscosity $M_c \approx 30\,000\ g\cdot mol^{-1}$. The zero shear viscosity of this PDMS at room temperature ($T = 22\ °C$) is $\eta_0 = 5$ Pa·s. Practically, MWCNTs and Sylgard 184-part A were mechanically mixed (1200 rpm) for 30 min at room temperature and used without any further mechanical treatment. The following concentration of MWCNTs in PDMS $\phi = 0.2\%$ has been then prepared for the present study. Further details about masterbatch and sample preparations can be found in the paper by Beigbeder et al.[35]

The viscoelastic and electrical measurements were carried out on an ARES rheometer (TA Instruments) at room temperature ($T \approx 22\ °C$). A specific geometry-cell has been developed in order to carry out combined rheological and dielectric measurements. The cell rheological geometry is constituted by isolated ring-plate electrodes connected to a frequency response analyzer HP4284. The upper and lower ring-plates have an inner diameter of 22 mm and an outer diameter of 25 mm. Thus, the strain difference between the inner and the outer part is only of 14%. This cell is actually a plate−plate geometry, where the sample is placed between the inner and outlet diameters of the upper and bottom ring shaped plates. Compared with a conventional plate−plate cell, such a ring-plate device allows us to apply a quasi-homogeneous shear rate and deformation throughout the sample volume (gap between the lower and upper ring-plates). The dielectric parameters conductivity and capacitance were recorded at a frequency of 1kHz in steady or oscillatory shearing mode by using specific connections to the experimental setup. Note that such type of device has been already developed and successfully used by Alig et al.[31]

Most of the rheological measurements were performed in an oscillatory shear mode (time or frequency sweep modes depending on the experiment) using the ring geometry. Specimens, which had been stored at room temperature for few days, were placed between the ring-surfaces. A film of approximately 0.7 mm thickness (h) was then deposited on the ring-plate surface. The upper ring-plate was brought in contact with the sample. Then, the sample was deformed by a steady downward displacement of the upper ring. When the sample was pressed to its final size (gap height between the rings, h_0, set to 0.5 mm) the displacement of the upper ring was stopped. The edge of the sample was then wiped off to remove squeezed out material. Consequently, the sample was initially submitted to a compressive deformation ($\varepsilon = \ln(h/h_0) \approx 0.34$) before the measurement. As the displacement speed was 5 mm.s^{-1}, an apparent compressive rate can be estimated at $\dot{\varepsilon} = 8.5\ s^{-1}$. Actually, the compressive rate changes in the range $\dot{\varepsilon} = 7.1\ s^{-1}$ to $\dot{\varepsilon} = 10\ s^{-1}$ during this squeezing experiment (the instantaneous compressive rate being $\dot{\varepsilon} = (1/H)(dH/dt)$). The purpose of the compressive step is to ensure the break

down of CNTs contacts under compressive rate as a posteriori checked (see Results and Discussion) by electrical and mechanical measurements. Our results will confirm that deformation and compressive rate are high enough to break up the CNTs network. Compared with experiments found in literature, we chose a compressive test rather than a shear test due to the fact that the latter is necessarily conducted after a squeezing deformation of the sample. To quantify the reformation of the CNTs network (we assumed a CNTs network in PDMS/MWCNTs samples stored for a few days) after compressive deformation, we performed time sweep experiments (combined electrical and dynamic measurements) at a mechanical frequency $\omega = 1\text{rad}\cdot\text{s}^{-1}$. The influence of dynamic shear deformation on the network recovery was then studied. This was the main scope of the present paper.

Moreover, in order to visualize the suspension evolution, some optical micrographs were taken using an optical microscope Orthoplan (Leitz) along time. The sample was placed between glass slides, undergoing a relatively high strain because of the inherent squeezing. Then successive pictures were recorded along time.

The suspension of finely dispersed MWCNTs (i.e., at the scale of CNTs entities) in the PDMS matrix can be regarded as a solution of rigid rods with aspect ratio L/d.[16] Defining ν as the number of CNTs per unit volume of solution, the dilute and semidilute regimes of concentration are delineated as follows.[37,38]

- Dilute regime: $\nu L^3 < 1$, the rods are able to rotate freely without any interference interaction with neighboring rods.
- Semidilute regime: $1/L^3 \ll \nu \ll 1/dL^2$), the rods are not able anymore to rotate freely without any interaction from surrounding ones. The transition from dilute to semidilute occurs when the rod concentration reach a value proportional to $1/L^3$. However, scaling developments showed that the rotational interference becomes significant when the transition is observed for $\nu \approx \beta/L^3$, where β is a dimensionless constant and experimentally close to $\beta \approx 30$. In terms of volume concentration ($\phi = (\pi/4)d^2L\nu$), the transition from dilute to semidilute regime of MWCNTs used in the present study is then $\phi_0 \approx (30\pi/4)(d/L)^2 \approx 0.1\%$. Our previous work[16] on linear viscoelasticity of MWCNTs confirmed experimentally that this concentration is the onset of the semidilute regime.

For concentrations such as $\nu > 1/dL^2$, the excluded volume of interaction can no longer be neglected. Just above the onset of this concentrated regime the solution remains isotropic at equilibrium (concentrated isotropic regime). Concerning the present MWCNTs, the onset of isotropic concentrated regime is around 0.5% and the nematic regime ($\nu > 4.2/dL^2$) would be higher than 2%. Finally, we can conclude from this analysis that the concentration used in the present study corresponds to the semidilute regime ($\phi = 0.2\%$, $\nu L^3 = 64$).

Results and Discussion

A measure of the relative importance of CNTs Brownian motion and compressive-induced deformation is quantitatively expressed by the dimensionless Peclet number $Pe = \dot{\epsilon}/D_r$ where D_r is the rotational diffusivity of the nanotubes (Brownian motion). Using the rotary diffusivity determined in our previous work,[16] we calculate $Pe \approx 10^5$ for $\phi = 0.2$. For $\phi = 0.5\%$ the Peclet number would tend to infinity $Pe \rightarrow \infty$. Consequently, the Brownian motion of CNTs is not a dominant mechanism and we can conclude that compressive rate controls the structure evolution of the CNTs. However, it can be assumed at this high Peclet number that nanotubes are randomly dispersed in PDMS liquid. Parts a–c of Figure 1 show the variation of the complex shear modulus

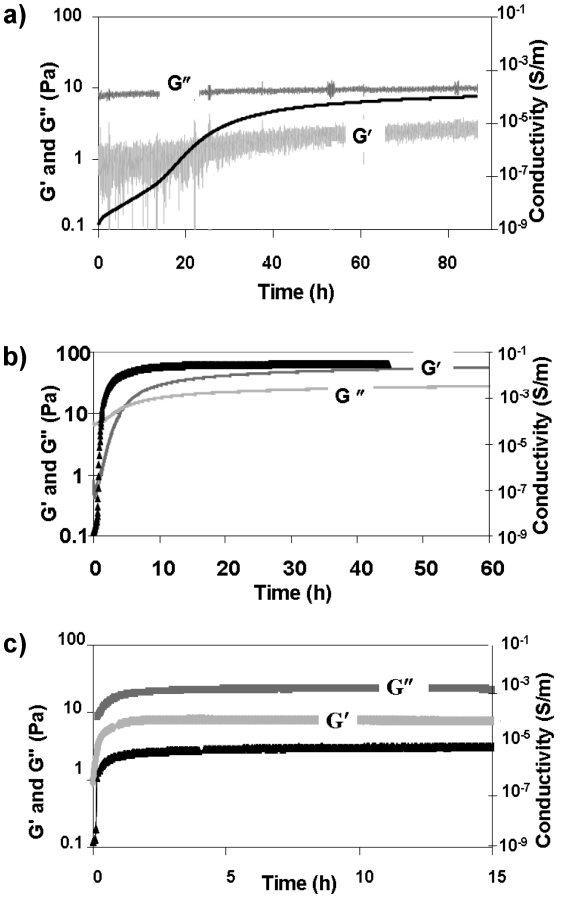

Figure 1. Study of the CNTs network just after a compressive deformation: Simultaneous time-resolved measurements of electrical conductivity and dynamic shear modulus under different strains ($\omega = 1$ rad·s^{-1}). $\gamma_0 = 5\%$ (a), 60% (b), and 200% (c).

($G^*(\omega) = G'(\omega) + jG''(\omega)$) and electrical conductivity in a time sweep experiment under different shear deformations ($\gamma_0 = 5$, 60, and 200%, respectively). First of all, these figures show that the conductivity of the composite, just after the compressive deformation, is close to the conductivity of the PDMS matrix ($\sigma < 10^{-9}\,\text{S}\cdot\text{m}^{-1}$) indicating the total destruction of the conductive CNTs network.

Under small deformation ($\gamma_0 = 5\%$), Figure 1a shows a weak variation of the complex shear modulus. The storage modulus is extremely noisy due to this low value of the applied deformation. On the contrary, the conductivity of the suspension increases progressively to reach $\sigma \approx 10^{-4}\,\text{S}\cdot\text{m}^{-1}$ after 48 h. This value is in the same order of magnitude as conductivity of usual semiconductive nanocomposites. In the present case, the Peclet number is close to $Pe \approx 10^5$ so that the Brownian motion of CNTs can be neglected compared to viscous forces even at $\gamma_0 = 5\%$. At this low deformation, the electrical property of the suspension varies from nonconductive to conductive behavior whereas the weak variation of the complex shear modulus does not show any network formation, at least at the frequency used. As suggested in many studies, the increase of the conductivity (over six decades in the present study) can be explained by the formation of a conductive network resulting from a mechanism of cluster aggregation. Furthermore, it has been pointed out in the literature[39,40] that the connectivity percolation (transfer of electric charge) occurs at lower concentration than rigidity percolation (elastic behavior). At the same concentration and dispersion/aggregation of CNTs, it can be then admitted that the variation of the electrical conductivity is more sensitive to the variation of the number of nanotube–nanotube contacts than

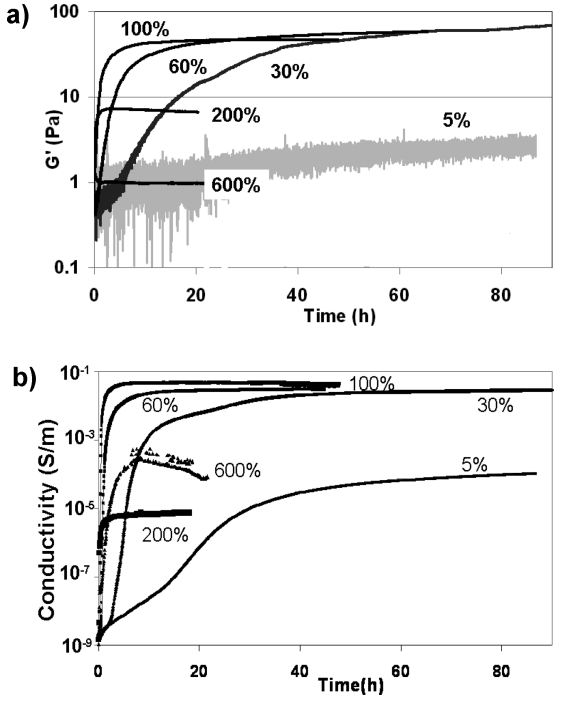

Figure 2. Variation of storage modulus (a) and variation of electrical conductivity (b) under different shear deformations: $\gamma_0 = 5, 30, 60, 100, 200$, and 600%.

the modulus, at least at the frequency used. In other words, the electrical conductivity method is much more sensitive than the mechanical one to characterize the cluster-aggregation mechanism.

Under the deformation of $\gamma_0 = 60\%$ (Figure 1b) the complex shear modulus and conductivity drastically increase with time. More precisely, the storage modulus increases within approximately 30 h from 0.5 to 60 Pa (two decades of variation) and the conductivity increases from 10^{-9}S.m^{-1} to 4×10^{-2} S·m^{-1} (more than seven decades of variation). On the other hand, the storage modulus crosses the loss modulus at $t \approx 5$ h ($\sigma \approx 5 \times 10^{-4}$ S·m^{-1}) showing that the elastic behavior of the suspension becomes dominant compared with the viscous behavior. Under the deformation of $\gamma_0 = 60\%$ (figure not plotted herein) the cross modulus was observed at $t \approx 1.5$ h ($\sigma \approx 2 \times 10^{-3}$ S·m^{-1}). This crossover can be associated with the formation of a CNTs network under the dynamic shear force. According to our previous work,[16] this network elasticity resulting from the nanotubes interactions appears to be a temporary elasticity. In other words, this transition does not obey the sol−gel transition as it depends on the frequency used.

Under higher deformation ($\gamma_0 = 600\%$, Figure 1c), the complex shear modulus and the conductivity rapidly increase but finally reach a much lower values ($G' \approx 1$ Pa and $\sigma \approx 10^{-4}$ S·m^{-1}). Actually, these results show a critical deformation. Beyond this critical deformation, the variation of the storage modulus and conductivity remains still accelerated but the final values considerably decreases with increasing the deformation. All the variations of the storage modulus and conductivity under different shear deformations ($\gamma_0 = 5, 30, 100, 200$, and 600%) are plotted in Figure 2, parts a and b, respectively. These figures clearly show that the variation of storage modulus and conductivity drastically accelerates with increasing the amplitude of the shear deformation up to a critical deformation close to $\gamma_c \approx 60\%$. In terms of the Peclet number $Pe = \gamma_0\omega/D_r$, its critical value is close to $Pe_c \approx 10^4$. This critical Peclet number is much lower than the Peclet number ($Pe \approx 10^5$) calculated for the compressive rate,

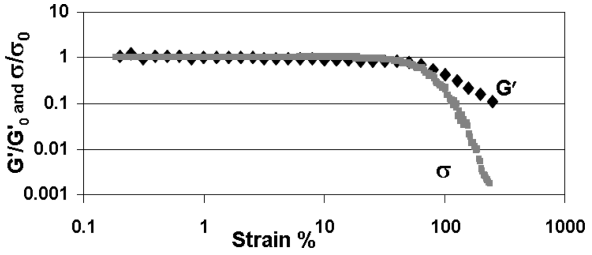

Figure 3. Variation of normalized storage modulus and electrical conductivity versus the deformation. The CNTs network was built under a shear deformation of 30%.

which confirms that this compressive-rate was high enough to completely breakdown the CNTs network. Beyond the critical deformation, the variation of the storage modulus and conductivity still accelerate but their steady values considerably decreases. However, within the deformation accessible in shear deformation ($\gamma_0 \approx 600\%$) the values of the modulus and conductivity do not return to the values obtained by the initial compressive deformation.

To check the critical value of the deformation, the famous effect of strain-amplitude dependence of the dynamic viscoelastic properties of filled polymers, generally referred as the Payne effect,[41] was studied. Figure 3 shows the variation of the reduced complex shear modulus and electrical conductivity versus the applied dynamic deformation ($\omega = 1$ rad·s^{-1}). This experiment was performed just after the time sweep experiment under the deformation $\gamma_0 = 30\%$. As expected, beyond the critical strain $\gamma_c = 60\%$, both storage modulus and electrical conductivity decrease with increasing the strain.

To sum up these results, the aggregation rate of CNTs (initially well dispersed in PDMS matrix) by a compressive deformation (semidilute regime) depends on the subsequent shear-dynamic regime. At low shear rate the CNTs aggregation rate increases with the shear dynamic rate until a critical value. Beyond this critical value, the level of network entanglement and/or contacts decrease as the shear rate increase. These observations are consistent with the works of Chatterjee and Krisnamoorti[25] who observed a stress overshoot under transient shear conditions. As discussed by the authors, this transient behavior can be explained in terms of the changing structure such as a cluster−cluster collision and CNTs network formation. In the same way, Hobbie and Fry[26] reported a universal phase diagram (mean cluster size versus stress) for the evolution from a solid-like network to flowing. On the other hand, Pegel et al.[42] qualitively concluded that the network structure is given by the balance of agglomerate growth and destruction under shear deformation. Finally, our results agree with the predictions of the model of Ma et al.[43] Their simulation showed that that low shear induced aggregation, but these aggregates broke down at high shear, forming small aggregates with less entanglement. This phenomenon of CNTs cluster aggregation under low shear was simply proved by optical microscopy (Figures 4a−c), which confirms our findings. Actually, the micrographs show no clear CNTs aggregates (some impurities may be spotted anyway) just after the compressive deformation. However, after a period (at rest) of a few hours, the aggregation (clustering mechanism) of the CNTs is clearly visible. It can be pointed out that the scale of this clustering is relatively high since it can be evidenced by simple optical microscopy. Finally, the cluster breakdown under compressive deformation and aggregation mechanism is clearly evidenced by Figure 5. Just after the compressive deformation, the variation of the complex shear modulus (under 5% strain) shows a rheological behavior close to the

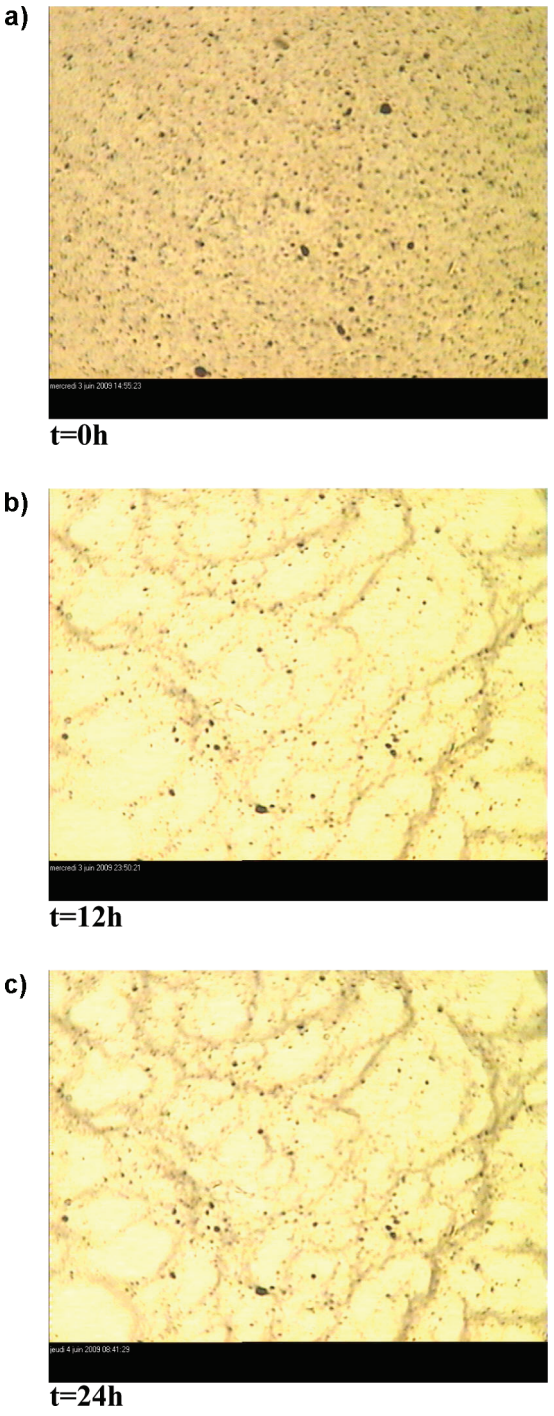

Figure 4. Optical observation of the aggregation of CNTs: (a) CNTs are well dispersed in PDMS matrix; (b and c) CNTs aggregate to build a network (picture width: 600 μm).

viscoelastic behavior of the PDMS matrix. This result proves that the CNTs network was destroyed under the compressive deformation. After aggregation process (under 60% strain, Figure 1b) the viscoelastic behavior of the composite shows a solid-like behavior, at least within the frequency bracket used in the present study, due to the formation of the CNTs network through dynamic CNTs aggregation. This result also confirms our previous results,[16] which showed the deviation of the scaling laws of the Doi−Edwards theory on rigid rods at CNTs concentrations higher than 0.12%. This deviation was related to a clustering phenomenon of MWCNTs that causes additional retarding of the rotational motion.

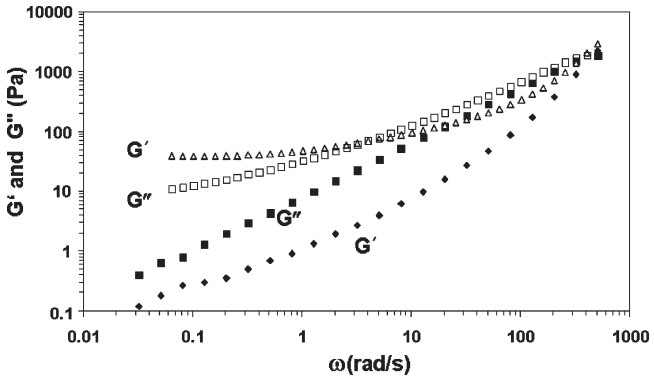

Figure 5. Variation of the complex shear modulus of the PDMS/CNTs suspension. Filled symbol: Viscoelastic behavior measured just after the compressive deformation. The nanotubes are supposed to be dispersed in the PDMS matrix. Unfilled symbols: Viscoelastic behavior measured at the end the aggregation process under $\gamma_0 = 30\%$.

Conclusion

The objective of the present work was to study the aggregation of untreated CNTs in a low-viscosity PDMS matrix from simultaneous time-resolved measurements of electrical conductivity and dynamic shear modulus under different strains. The concentration of nanotubes ($\phi = 0.2\%$) was chosen in order to be in the semidilute regime of the suspensions.

It was shown that the kinetics of CNTs aggregation strongly depend on the amplitude of the dynamic shear deformation. Actually, the kinetics of aggregation increases with increasing the deformation. However, above a critical deformation $\gamma_c = 60\%$ at $\omega = 1$ rad·s^{-1} (corresponding to a critical Peclet number $Pe_c \approx 1 \times 10^4$), the equilibrium value of the storage modulus and electrical conductivity decreases with increasing the deformation. As far as we know, it is the first time that such mechanism is clearly proved under dynamic conditions. Note that analogous behaviors under steady shear flow have been previously reported by Hobbie and Fry[26] and Ma et al.[27] Furthermore, this phenomenon of CNTs cluster aggregation was also highlighted by optical microscopy as the clustering mechanism of the CNTs can be seen after few hours.

Finally, these results show that the CNTs network formed by aggregation destroys under high deformation; from a viscoelastic point of view, this critical deformation can be associated with the transition between linear and nonlinear regime (Payne effect).

References and Notes

(1) Mitchell, C. A.; Bahr, J. L.; Arepalli, S.; Tour, J. M.; Krishnamoorti, R. *Macromolecules* **2002**, *35*, 8825–8830.
(2) Hough, L. A.; Islam, M. F.; Janmey, P. A.; Yodh, A. G. *Phys. Rev. Lett.* **2004**, *93* (16), 168102.
(3) Pötschke, P.; Abdel-Goad, M.; Alig, I.; Dudkin, S.; Lellinger, D. *Polymer* **2004**, *45*, 8863–8870.
(4) Du, F.; Scogna, R. C.; Zhou, W.; Brand, S.; Fischer, J. E.; Winey, K. I. *Macromoloecules* **2004**, *37*, 9048–9055.
(5) Kharchenko, S. B.; Douglas, J. F.; Obrzut, J.; Grulke, E. A.; Migler, K. B. *Nat. Mater.* **2004**, *3*, 564–568.
(6) Zhang, Q.; Lippits, D. R.; Rastogi, S. *Macromolecules* **2006**, *39*, 658–666.
(7) Chatterjee, T.; Krishnamoorti, R. *Phys. Rev. E* **2007**, *75*, 050403.
(8) Wang, M.; Wang, W.; Liu, T.; Zhang, W. D. *Compos. Sci. Technol.* **2008**, *68*, 2408–2502.
(9) Xu, D. H.; Wang, Z. H.; Douglas, J. F. *Macromolecules* **2008**, *41*, 815–825.
(10) Chatterjee, T.; Jackson, A.; Krishnamoorti, R. *J. Am. Chem. Soc.* **2008**, *130*, 6934–6935.
(11) Zhang, Q.; Fang, F.; Zhao, X.; Li, Y.; Zhu, M.; Chen, D. *J. Phys. Chem. B* **2008**, *112*, 12606–12611.

(12) Lima, M. D.; Andrade, M. J.; Skakalova, V.; Bergmann, C. P.; Roth, S. *J. Mater. Chem.* **2007**, *17*, 4846–4853.
(13) Deng, F.; Zheng, Q. S. *Appl. Phys. Lett.* **2008**, *92*, 071902.
(14) Hu, N.; Masuda, Z.; Yan, C.; Yamamoto, G.; Fukunaga, H.; Hashida, T. *Nanotechnology* **2008**, *19*, 215701.
(15) Kayatin, M. J.; Davis, V. A. *Macromolecules* **2009**, *42*, 6624–6632.
(16) Marceau, S.; Dubois, Ph; Fulchiron, R.; Cassagnau, P. *Macromolecules* **2009**, *42*, 1433–2438.
(17) Tuteja, A.; Mackay, M. E.; Hawker, C. J.; Van Horn, B. *Macromolecules* **2005**, *38*, 8000–8011.
(18) Jain, S.; Goossens, J. G. P.; Peters, G. W. M.; van Duin, M.; Lemstra, P. J. *Soft Matter* **2008**, *4*, 1848–1854.
(19) Vega, J. F.; Martinez-Salazar, J.; Trujillo, M.; Arnal, M. L.; Muller, A. J.; Bredeau, S.; Dubois, Ph *Macromolecules* **2009**, *42*, 4719–4727.
(20) Hobbie, E. K.; Wang, H.; Kim, H.; Lin-Gibson, S.; Grulke, E. A. *Phys. Fluids* **2003**, *15*, 1196–1202.
(21) Hobbie, E. K.; Wang, H.; Kim, H.; Han, C. C.; Grulke, E. A.; Obrzut, J. *Rev. Sci. Instrum.* **2003**, *74*, 1244–1250.
(22) Fry, D.; Langhorst, B.; Kim, H.; Grulke, E.; Wang, H.; Hobbie, E. H. *Phys. Rev. Lett.* **2005**, *95*, 038304.
(23) Fry, D.; Langhorst, B.; Wang, H.; Becker, M. L.; Bauer, B. J.; Grulke, E. A.; Hobbie, E. K. *J. Chem. Phys.* **2006**, *124*, 054703.
(24) Wang, H.; Christopherson, G. T.; Xu, Z. Y.; Porcar, L.; Ho, D. L.; Hobbie, E. K. *Chem. Phys. Lett.* **2005**, *416*, 182–186.
(25) Chatterjee, T.; Krishnamoorti, R. *Macromolecules* **2008**, *41*, 5333–5338.
(26) Hobbie, E. K.; Fry, D. J. *Phys. Rev. Lett.* **2006**, *97*, 036101.
(27) Ma, A. W. K.; Mackley, M. R.; Rahatekar, S. S. *Rheol. Acta* **2007**, *46*, 979–987.
(28) Pötschke, P.; Dudkin, S. M.; Alig, I. *Polymer* **2003**, *44*, 5023–5030.
(29) Alig, I.; Lellinger, D.; Engel, M.; Skipa, T.; Potschke, P. *Polymer* **2008**, *49*, 1902–1909.
(30) Leboeuf, M.; Ghamri, N.; Brulé, B.; Coupez, T.; Vergnes, B. *Rheol. Acta* **2008**, *47*, 201–212.
(31) Alig, I.; Lellinger, D.; Dukin, S.; Potschke, P. *Polymer* **2007**, *48*, 1020–1029.
(32) Obrzut, J.; Douglas, J. F.; Kharchenko, S. B.; Migler, K. B. *Phys Rev B* **2007**, *76*, 195420.
(33) Alig, I.; Skipa, T.; Lellinger, D.; Potschke, P. *Polymer* **2008**, *49*, 3524–3532.
(34) Huang, Y. Y.; Ahir, S. V.; Terentjev, E. M. *Phys Rev B* **2006**, *73*, 125422.
(35) Beigbeder, A.; Linares, M.; Devalckenaere, M.; Degée, P.; Claes, M.; Beljonne, D.; Lazzaroni, R.; Dubois, Ph. *Adv. Mater.* **2008**, *20*, 1003–1007.
(36) Ressia, J. A.; Villar, M. A.; Vallés, E. M. *Polymer* **2000**, *41*, 6885–6894.
(37) Doi, M., Edwards, S. F. *The theory of polymer dynamics*; Oxford Press: London, 1986
(38) Larson, R. G. *The structure and rheology of complex fluids*; Oxford University Press: London, 1999.
(39) Kantor, Y.; Webman, I. *Phys. Rev. Lett.* **1984**, *52*, 1891–1894.
(40) Latva-Kokko, Timonen J. *Phys Rev. E* **2001**, *64*, 000117.
(41) Payne, A. R. *Reinforcement of Elastomers*; Interscience:New York, 1965, Chapter 3, pp 69−123
(42) Pegel, S.; Pötschke, P.; Petzold, G.; Alig, I.; Dudkin, S. M.; Lellinger, D. *Polymer* **2008**, *49*, 974–984.
(43) Ma, W. K. A.; Chinesta, F.; Ammar, A.; Mackley, M. R. *J. Rheol.* **2008**, *52*, 1311–1330.